

## **Discovery of Fe<sub>2</sub>P-type Ti(Zr/Hf)<sub>2</sub>O<sub>6</sub> Photocatalysts toward Water Splitting**

Xiangying Meng<sup>1,\*</sup>, Lu Wang<sup>1</sup>, Dongyan liu<sup>1</sup>, Xiaohong Wen<sup>1</sup>, Qiang Zhu<sup>2,\*</sup>,  
William A. Goddard III<sup>3</sup>, Qi An<sup>3</sup>

<sup>1</sup>College of Sciences, Northeastern University, Shenyang 110819, China

<sup>2</sup>Department of Geosciences and Department of Physics and Astronomy, State University of New  
York, Stony Brook, NY 11794-2100, United States

<sup>3</sup>Materials and Process Simulation Center, California Institute of Technology, Pasadena, CA  
91125, United States

\*Correspondence and requests for materials should be addressed to X. Y. Meng or Q. Zhu (Email:  
x\_y\_meng@mail.neu.edu.cn; qiang.zhu@stonybrook.edu)

## 1. The crystallographic information (in .cif format) for TiZr<sub>2</sub>O<sub>6</sub>

# CRYSTAL DATA

#-----

data\_VESTA\_phase\_1

_pd_phase_name	'TiZr2O6'
_cell_length_a	5.59950
_cell_length_b	5.59950
_cell_length_c	3.16899
_cell_angle_alpha	90
_cell_angle_beta	90
_cell_angle_gamma	120
_symmetry_space_group_name_H-M	'P -6 2 m'
_symmetry_Int_Tables_number	189

loop\_

\_symmetry\_equiv\_pos\_as\_xyz

'x, y, z'  
'-y, x-y, z'  
'-x+y, -x, z'  
'x, y, -z'  
'-y, x-y, -z'  
'-x+y, -x, -z'  
'y, x, -z'  
'x-y, -y, -z'  
'-x, -x+y, -z'  
'y, x, z'  
'x-y, -y, z'  
'-x, -x+y, z'

loop\_

\_atom\_site\_label

\_atom\_site\_occupancy

\_atom\_site\_fract\_x

\_atom\_site\_fract\_y

\_atom\_site\_fract\_z

\_atom\_site\_adp\_type

\_atom\_site\_U\_iso\_or\_equiv

\_atom\_site\_type\_symbol

O1	1.0	0.750790	0.750790	0.000000	Uiso	0.012670	O
O4	1.0	0.597320	0.000000	0.500000	Uiso	0.012670	O
Ti1	1.0	-0.000000	-0.000000	0.500000	Uiso	0.012670	Ti
Zr1	1.0	0.666667	0.333333	0.000000	Uiso	0.012670	Zr

## 2. The crystallographic information (in .cif format) for TiHf<sub>2</sub>O<sub>6</sub>

# CRYSTAL DATA

#-----

data\_VESTA\_phase\_1

_pd_phase_name	'TiHf2O6'
_cell_length_a	5.54699
_cell_length_b	5.54699
_cell_length_c	3.15185
_cell_angle_alpha	90
_cell_angle_beta	90
_cell_angle_gamma	120
_symmetry_space_group_name_H-M	'P -6 2 m'
_symmetry_Int_Tables_number	189

loop\_

\_symmetry\_equiv\_pos\_as\_xyz

'x, y, z'  
'-y, x-y, z'  
'-x+y, -x, z'  
'x, y, -z'  
'-y, x-y, -z'  
'-x+y, -x, -z'  
'y, x, -z'  
'x-y, -y, -z'  
'-x, -x+y, -z'  
'y, x, z'  
'x-y, -y, z'  
'-x, -x+y, z'

loop\_

\_atom\_site\_label

\_atom\_site\_occupancy

\_atom\_site\_fract\_x

\_atom\_site\_fract\_y

\_atom\_site\_fract\_z

\_atom\_site\_adp\_type

\_atom\_site\_U\_iso\_or\_equiv

\_atom\_site\_type\_symbol

O1	1.0	0.256440	0.256440	0.500000	Uiso	0.012670 O
O4	1.0	0.406850	0.000000	-0.000000	Uiso	0.012670 O
Ti1	1.0	-0.000000	0.000000	0.000000	Uiso	0.012670 Ti
Hf1	1.0	0.666667	0.333333	0.500000	Uiso	0.012670 Hf

### 3. The elastic constants and modulus of Ti (Zr/Hf)<sub>2</sub>O<sub>6</sub>

Based on the energy-strain relations, the independent elastic constants of Ti(Zr/Hf)<sub>2</sub>O<sub>6</sub> at the zero-pressure are calculated and listed in Table 1s. It is clear that the calculated elastic constants of Ti(Zr/Hf)<sub>2</sub>O<sub>6</sub> fulfill the mechanical stability criteria:  $C_{44} > 0$ ,  $C_{11} > |C_{12}|$ , and  $(C_{11} + C_{12})C_{33} > 2C_{12}^2$ .

### 4. The phonon dispersion curves at 0 GPa of Fe<sub>2</sub>P-type ZrO<sub>2</sub> and HfO<sub>2</sub>

In Fig. 1s\_a, no imaginary phonon frequency is observed in Fe<sub>2</sub>P-type ZrO<sub>2</sub> at 0 GPa, indicating its dynamical instability at ambient conditions. However, in Fe<sub>2</sub>P-type HfO<sub>2</sub> (Fig. 1s\_b), an acoustic phonon branch is found negative. The dynamical stability of Fe<sub>2</sub>P-type at ambient conditions need to be further investigated by both theoretical and experimental studies.

### 5. HSE band structures at 0 GPa of Fe<sub>2</sub>P-type ZrO<sub>2</sub> and HfO<sub>2</sub>

HSE obtained band structures of ZrO<sub>2</sub> and HfO<sub>2</sub> are shown in Fig. 2s. The present calculations give bandgaps of 2.64 eV and 3.00 eV for Fe<sub>2</sub>P-type ZrO<sub>2</sub> and HfO<sub>2</sub>, respectively. The ionicity for the Fe<sub>2</sub>P-type compounds is listed in Table 2s. The bandgap of Fe<sub>2</sub>P-type IVa-oxides is found to be wider and wider with the increase of the ionicity.

**Table S1.** The independent elastic constants and modulus (bulk modulus  $B$ , shear modulus  $G$ , Young's modulus  $E$ , and Poisson's ratio  $\nu$ ) of Ti(Zr/Hf)<sub>2</sub>O<sub>6</sub>. All elastic parameters except  $\nu$  are in GPa.

	$C_{11}$	$C_{33}$	$C_{44}$	$C_{66}$	$C_{12}$	$C_{13}$	$B$	$G$	$E$	$\nu$	$B/G$
TiZr <sub>2</sub> O <sub>6</sub>	458	424	124	124	250	175	281	115	305	0.32	2.43
TiHf <sub>2</sub> O <sub>6</sub>	475	442	132	102	269	177	291	119	314	0.32	2.45

**Table S2.** The ionicity and HSE bandgap (eV) of Fe<sub>2</sub>P-type IVa-oxides.

	TiO <sub>2</sub>	TiZr <sub>2</sub> O <sub>6</sub>	ZrO <sub>2</sub>	TiHf <sub>2</sub> O <sub>6</sub>	HfO <sub>2</sub>
Ionicity	39%	42%	44%	45%	48%
HSE Bandgap	2.00	2.29	2.64	2.65	3.00

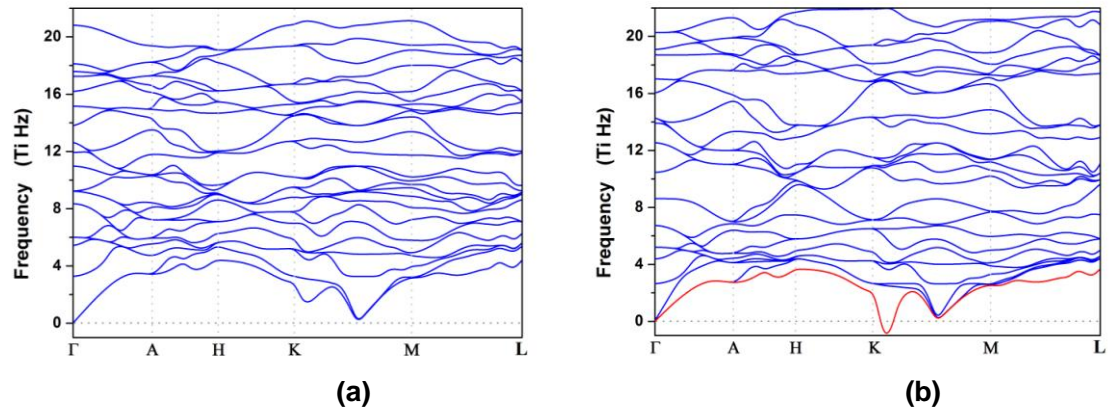


**Figure S1.** Phonon dispersion curves for Fe<sub>2</sub>P-type ZrO<sub>2</sub> (a) and HfO<sub>2</sub> (b) at 0 GPa

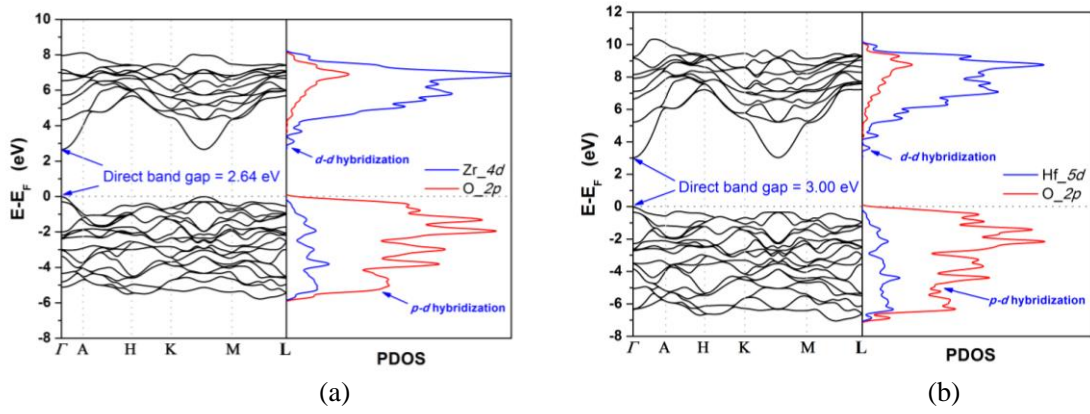


**Figure S2.** HSE band structure of Fe<sub>2</sub>P-type ZrO<sub>2</sub> (a) and HfO<sub>2</sub> (b) at 0 GPa